Estimation of Soil Profile Physical and Chemical Properties Using a VIS-NIR-EC-Force Probe

Yongjin Cho[1] and Kenneth A. Sudduth[2]

[1]Bioengineering Department, University of Missouri, Columbia, Missouri

[2]USDA-ARS Cropping Systems and Water Quality Research Unit, Columbia, Missouri

A paper from the Proceedings of the
13th International Conference on Precision Agriculture
July 31 – August 4, 2016
St. Louis, Missouri, USA

Abstract. *Combining data collected in-field from multiple soil sensors has the potential to improve the efficiency and accuracy of soil property estimates. Optical diffuse reflectance spectroscopy (DRS) has been used to estimate many important soil properties, such as soil carbon, water content, and texture. Other common soil sensors include penetrometers that measure soil strength and apparent electrical conductivity (EC_a) sensors. Previous field research has related those sensor measurements to soil properties such as bulk density, water content, and texture. A commercial instrument that can simultaneously collect reflectance spectra, EC_a and soil strength data is now available. The objective of this research was to relate laboratory-measured soil properties, including bulk density, carbon, water content, and texture fractions to sensor data from this instrument. At four field sites in mid-Missouri, profile sensor measurements were obtained to 0.9 m followed by collection of soil cores at each site for laboratory measurements. Using only reflectance data, soil bulk density, total organic carbon, and water content were not well-estimated (R^2 = 0.32, R^2 = 0.67, and R^2 = 0.40, respectively). Adding EC_a and soil strength data provided only a slight improvement in water content estimation (R^2 = 0.47) and little to no improvement in BD and TOC estimation. When data were analyzed separately by Major Land Resource Area (MLRA), fusion of data from all sensors did improve soil texture fraction estimates. The largest improvement compared to VIS-NIR reflectance alone was for MLRA 115B, where estimation errors were reduced by approximately 14 to 26%. This study showed promise for in-field sensor measurement of some soil properties. Additional field data collection and model development are needed for those soil properties where combination of data from multiple sensors is required.*

Keywords. *Precision agriculture, NIR spectroscopy, soil properties, reflectance spectra, soil sensing.*

Introduction

Precision agriculture is a management system where field operations and application of chemicals such as fertilizers, pesticides, and herbicides are matched to actual point-by-point needs within fields, providing economic benefits to farmers and protection of the soil environment from excessive chemical application. For precision agriculture to achieve its goals, site-specific quantification of soil physical and chemical properties that affect soil quality and crop production is necessary. Some properties for which site-specific quantification is needed include soil texture, bulk density, water content, and organic matter (or organic carbon). All of these have been shown to vary considerably either across landscapes, with depth, or both. Additionally, all of these properties are important in one or more processes critical for crop production and ecosystem services.

Diffuse reflectance spectroscopy (DRS) is one promising, nondestructive soil sensing technique. Many investigators have successfully estimated soil physical and chemical properties in the laboratory using DRS in the visible (VIS; 400-700 nm), near-infrared (NIR; 700-2500 nm), and mid-infrared (MIR; 2500-25000 nm) wavelength ranges. In addition, several DRS soil sensors have been successfully used in field settings (Kusomo et al., 2008; Kweon et al., 2008; Mouazen et al., 2007).

To date, most DRS soil sensing research has been carried out in the VIS, NIR, or combined VIS-NIR wavelength ranges. Viscarra Rossel et al. (2006) provided a comprehensive review of soil DRS applications, including accuracy statistics. Many researchers have used DRS to estimate soil carbon (or soil organic matter) and soil water content (WC), generally with good success. For example, Sudduth and Hummel (1993) estimated organic matter (R^2 = 0.89) and water content (R^2 = 0.94) for 30 Illinois surface soils prepared to a range of moisture tension levels. Mouazen et al. (2007) estimated total C (R^2 = 0.73) and water content (R^2 = 0.89) using samples representative of Belgian soils. Lee et al. (2009) analyzed surface and whole-profile datasets obtained from ten fields in five states of the U.S. Corn Belt. Soil organic carbon was well estimated for both surface (R^2 = 0.87) and profile (R^2 = 0.80) data. Total C estimates were not as good (R^2 ≤ 0.65), likely due to interference from inorganic carbonate C at some sites. Chang et al. (2001) estimated total C (R^2 = 0.87, RMSE = 7.86 g kg^{-1}), water content (R^2 = 0.84, RMSE = 0.5 g kg^{-1}), clay content (R^2 = 0.67, RMSE = 4.06%), sand content (R^2 = 0.82, RMSE = 11.93%), and silt content (R^2 = 0.84, RMSE = 9.51%) for surface and subsurface soils obtained from across the US in the VIS-NIR spectral range using principal components regression (PCR). When using partial least squares regression (PLSR), Chang and Laird (2002) similarly estimated total C (R^2 = 0.91, RMSE = 0.65 g kg^{-1}) in the VIS-NIR spectral range. Shepherd and Walsh (2002) successfully estimated clay content (R^2 = 0.78, RMSE = 7.5 g kg^{-1}), sand content (R^2 = 0.76, RMSE = 10.8 g kg^{-1}), and silt content (R^2 = 0.67, RMSE = 4.9 g kg^{-1}) for archived topsoils from eastern and southern Africa. In contrast, there are few reports of using reflectance data to estimate soil bulk density (BD). In a recent study Askari et al. (2015) reported good results for both total core BD (R^2 = 0.81) and BD of the soil particles smaller than 2 mm (R^2 = 0.73).

Additionally, some researchers have simulated in-situ spectroscopy by using laboratory spectrometers to collect data from soil cores. This approach was used to estimate soil C and N by Kusumo et al. (2008) and to estimate total C by Morgan et al. (2009). Morgan et al. (2009) compared data from field-moist soil to data from dried and sieved samples and found only a slight decrease in accuracy with data from the field-moist soil. A commercial instrument, the Veris P4000 (Veris Technologies, Salina, KS) has recently become available that allows in-situ collection of VIS-NIR data to a depth of 1 m (Christy et al., 2011). Kweon et al. (2008) used this probe to collect data on six Kansas fields and reported R^2 values ranging from 0.69 to 0.89 for soil C estimation. Hodge and Sudduth (2012) compared the accuracy of the Veris P4000 VIS-NIR spectrometer operating in

bench-top mode with its accuracy in field probe spectrometer mode. Total C estimation was more accurate in the laboratory (R^2 = 0.93 to 0.96) than in the field (R^2 = 0.78 to 0.90) in the 1302-2202 nm range.

Another promising soil sensing technique is measurement of apparent electrical conductivity (EC_a), which responds to a number of important soil physical and chemical properties, including salinity, clay content, cation exchange capacity (CEC), clay mineralogy, soil pore size and distribution, and soil moisture content (McNeill, 1992). A theoretical basis for the relationship between EC_a and soil properties was developed by Rhoades et al. (1989). In this model, EC_a was defined as a function of soil water content, the electrical conductivity of the soil water, soil bulk density, and the electrical conductivity of the soil particles.

Most soil EC_a data collection is done with mobile sensors that can map the apparent conductivity over a soil depth interval that is usually 30 cm or greater. An example of such a mobile sensor is the Veris 3100/3150 that uses six rolling coulters for electrodes and provides two simultaneous EC_a measurements (Lund et al., 1999). In addition to the widely used proximal EC_a sensors, there are commercial penetrometer-based sensors that allow direct measurement of EC_a as a function of depth (Kweon et al., 2008; Sudduth et al., 2004), providing data on a narrow depth interval. Application of a penetrometer-type EC_a sensor to better understand soil profile variability was described by Myers et al. (2010). Sudduth et al. (2013) combined data from proximal and penetrometer EC_a sensors to improve modeling of conductivity–depth relationships in terms of model selection, model parameterization, and model calibration.

Soil compaction can be naturally occurring or caused by forces exerted on the soil during field operations, and the degree of compaction can be influenced by soil properties such as texture and water content. Thus, the degree of compaction can vary among within-field locations, and/or among different soil horizons due to their specific soil conditions (Koolen and Kuipers, 1983). Therefore, site-specific, three-dimensional quantification of variations in compaction is an important part of an overall precision management plan. Although compaction may be more directly quantified by laboratory determination of related soil properties (e.g., dry bulk density), the common approach for field use is to measure soil strength. The main tool used to quantify soil strength by depth and thereby provide information related to soil compaction and morphological characteristics is the cone penetrometer (Mulqueen et al., 1977). The index of soil strength measured by a cone penetrometer, cone index (CI, in kPa), is defined as the force per unit base area required to push the penetrometer through a specified small increment of soil (ASAE, 2005). Major factors affecting CI or soil strength include water content, bulk density, and clay content of the soil (Elbanna and Witney, 1987, Chung et al., 2008).

Many soil sensors, including those measuring reflectance, soil strength (CI) and EC_a, respond to a number of different soil properties, as described above. Because of this, it is often difficult to quantify soil properties with data from a single sensor. For improved results, a data fusion or sensor fusion approach (Adamchuk et al., 2011) could be used. For example, BD estimates based on EC_a were improved when CI data were added and were further improved when WC estimates were included as candidate variables in the model (Cho et al., 2014). One commercial instrument providing sensor fusion capability is the Veris P4000 VIS-NIR-force probe. Recent reports describe use of the Veris P4000 in various research situations. Piikki et al. (2014) used data from the P4000 along with mobile proximal sensor data to implement three-dimensional digital soil mapping. Matney et al. (2014) related P4000 data to archaeological features at Native American settlement sites. Wetterlind et al. (2015) estimated soil texture and soil organic matter (SOM) content with estimation errors of around 6% for clay and silt, 10–11% for sand and 0.3–0.5% for SOM. The best single data source was VIS-NIR reflectance, and the small improvements obtained by combining sensors did not provide strong support for combining VIS-NIR measurements with measurements of EC_a and or CI. As only a few previous studies have been reported, there is a need to evaluate the performance of the P4000 under different field conditions and for additional soil properties.

Objectives

The objective of this research was to relate the soil properties of bulk density (BD), total soil organic carbon (TOC), soil water content (WC), and soil texture fractions to soil EC_a, soil strength as CI, and soil spectral reflectance as measured by the Veris P4000 VIS-NIR-EC-force probe. Specific objectives were to:

1. Assess the accuracy of VIS-NIR spectral reflectance alone for estimating soil properties for the entire profile across multiple soils, using partial least squares (PLS) regression methods.
2. Compare using multiple independent variables (VIS-NIR, EC_a, and CI) to estimate soil properties with using VIS-NIR reflectance alone.

Materials and methods

Field sites

Data were obtained from fields in central Missouri, USA. Table 1 gives the locations and general characteristics of the four fields. The soils at field 1 were primarily of the Putnam and Mexico series. Surface texture was silt loam and the subsoil horizons were silty clay loam and silty clay. The soils at field 2 were of the Leonard series. Surface texture was silt loam and the subsoil claypan horizon was silty clay loam. The soils at field 3 were primarily of the Armstrong and Mexico series. Surface textures ranged from silt loam to loam, and the subsoil claypan horizon was silty clay loam and clay loam. The soils at field 4 were of the Wrengart series and textures were silt loam over silty clay loam. The 4 fields are included in 2 different "major land resource areas" (MLRA), as defined by the U.S. Department of Agriculture (1981). Major land resource areas are geographic areas that are characterized by a particular pattern of soils, climate, water resources and land uses. Thus, it would be reasonable to expect that the soil characteristics of fields 1, 2, and 3 (MLRA 113) would be more similar to each other than the soil characteristics of field 4 (MLRA 115B).

Table 1. Study fields characteristics.

Field	No. measured location	Size (ha)	Major Land Resource Area	Predominant Soils	Location
1	5	37.5	113 Central Claypan Areas	Putnam and Mexico	39.35 N, 92.43 W
2	6	3.8	113 Central Claypan Areas	Leonard	39.19 N, 92.20 W
3	3	9.4	113 Central Claypan Areas	Armstrong and Mexico	39.00 N, 92.11 W
4	8	9.4	115B Central Mississippi Valley Wooded Slopes, Western Part	Wrengart	38.58 N, 92.40 W

Data collection and processing

Spectral data were collected in April, 2012 with the Veris P4000 VIS-NIR-EC-force probe (figure 1) at three to eight locations in each of the four study fields (table 1). The probe measured VIS-NIR reflectance through a sapphire window, EC_a (mS m^{-1}) from dipole contacts, and CI (kPa) from a load cell force sensor. The P4000 used a Si CCD array spectrometer and an InGaAs photodiode-array spectrometer to collect VIS and NIR measurements in the range of 343-2202 nm. Dark current and reflectance standard calibration were performed according to manufacturer's recommendations (Kweon et al., 2008). P4000 measurements (VIS-NIR, CI, and EC_a) were obtained at a nominal 20 Hz rate as the probe was hydraulically lowered into the soil to at least 90 cm depth. Output data from the system were an average of 25 raw measurements and were obtained on approximately 6 to 7 cm depth increments.

Calibration soil samples were obtained from each location using a hydraulic soil coring machine. Cores for TOC, BD, WC, and texture were divided into four segments with narrower intervals nearer the surface (i.e., 0-15 cm, 15-30 cm, 30-60 cm, and 60-90 cm) to provide better discrimination in surface soil layers. Samples were analyzed for TOC with a LECO C Analyzer (LECO Corp., St.

Joseph, MI) using standard dry combustion analysis procedures (Nelson & Sommers, 1996). Soil bulk density was determined by the cylinder method knowing the diameter and length of the core. Water content was determined gravimetrically by oven drying and soil texture fractions (clay, silt, and sand) were determined by the sieve-pipette method (Gee and Bauder, 1986).

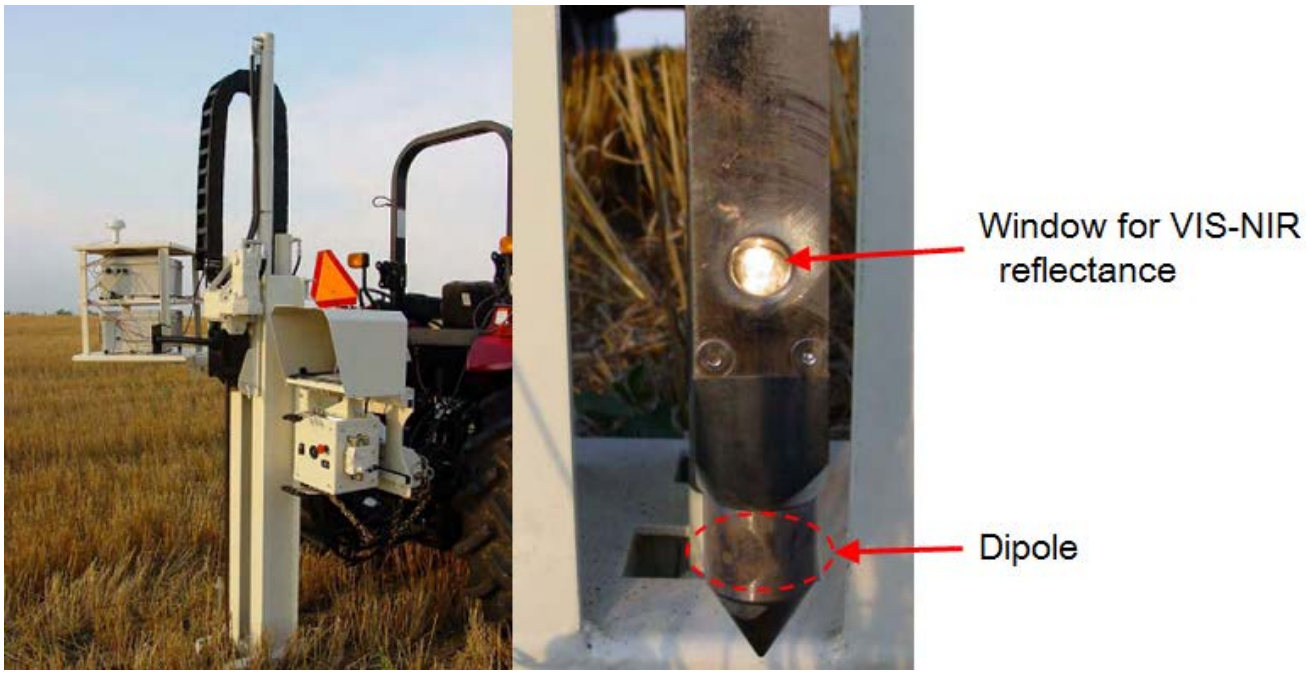

Figure 1. Veris P4000 VIS-NIR-EC-force instrument (left) and closeup view of P4000 probe tip (right).

Analytical procedures

As soil and sensor data were collected on different depth increments, it was necessary to combine them to a common level of spatial support. This was done using weighted averaging of the sensor data to match the soil sample cores at the 0-15, 15-30, 30-60 and 60-90 cm depths. The weighting procedure was based upon the fact that the sensor depth recorded is the final depth of the instrument at the end of the 25 scan observation period. This depth then defines the starting depth for the next observation in the probing sequence. These depth segments varied somewhat in thickness, with an average thickness of 6.7 cm and a standard deviation of approximately 1 cm. Because the initial starting depth for the first observation in any probe was unknown, we chose for the first scan to start at depth of zero, or at a depth such that the first observation represented no more than 6.7 cm of depth. For NIR spectral, EC_a and CI data, observations which fell entirely into a single target layer were weighted by the depth increment of an observation into that layer. Where observations spanned two soil layers, the observation was weighted into both layers, based upon the amount of depth represented in each layer. At the end of this procedure, the weighted average sensor data (spectral, EC_a, and CI) were merged with the corresponding soils data (BD, TOC, WC, and texture).

Spectral data were preprocessed to improve stability of the regression. The first 10 readings at the lower visible wavelengths were deleted due to their low signal-to-noise ratio; thus, the revised spectra began at 402 nm (figure 2). Each spectral scan was (1) transformed from reflectance to absorbance (log10 [1/reflectance]), (2) subjected to a standard normal variate transform (i.e., every data point of the spectra (402-2220 nm) is subtracted from the mean and divided by the standard deviation), and (3) smoothed with a 10-point (nominally 49 nm) moving average. These preprocessing steps were chosen because they gave good results in a preliminary analysis investigating various preprocessing treatments (data not shown). The standard normal variate approach was used to remove the multiplicative interferences of scatter and particle size (Barnes et al., 1989).

Partial least squares (PLS) regression implemented in Unscrambler version 10.1 (CAMO, Inc., Oslo, Norway) was used to develop calibrations between soil properties and spectra. PLS has been widely used in chemometrics, remote sensing, and spectral data processing to deal with large datasets containing highly correlated variables. A 20-fold cross validation procedure was used to select the number of PLS factors to use in the regression, increasing predictive capability and decreasing the potential for overfitting. Model evaluation was based on coefficient of determination (R^2), root mean square error of prediction (RMSEP), and the ratio of standard deviation to RMSEP (RPD). RPD is useful when comparing results from datasets containing different degrees of variability. Chang et al. (2001), Saeys et al. (2005), and Lee et al. (2009) suggested that, as a general guideline, RPD > 2.0 or R^2 > 0.8 indicates good estimation of soil properties, 0.65 < R^2 < 0.80 or 1.5 < RPD < 2.0 indicates fair estimation, and RPD < 1.4 or R^2 < 0.5 indicates poor estimation.

Using PLS regression, four different models were developed for each soil property, based on different combinations of independent data: (1) VIS-NIR reflectance alone, (2) VIS-NIR+EC_a, (3) VIS-NIR+CI, and (4) VIS-NIR+EC_a+CI. In addition, SMLR was used to relate EC_a and CI, alone and in combination, to each soil property.

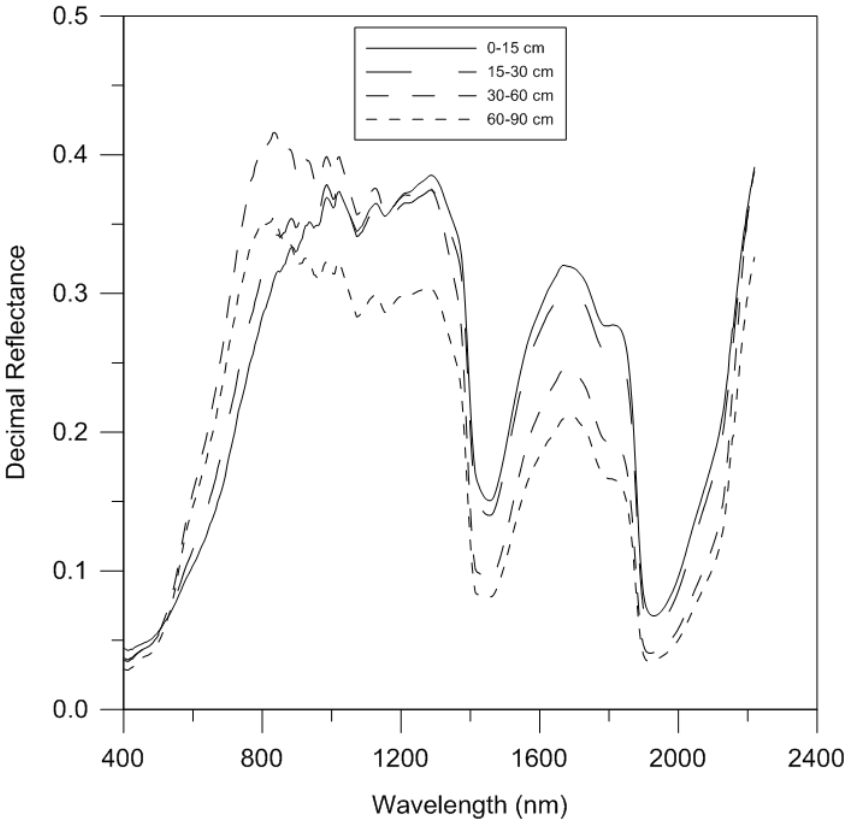

Figure 2. Soil reflectance spectra for the four soil depths at one sampling site.

Results and discussion

Descriptive statistics of soil properties

Means and standard deviations of soil properties (TOC, WC, and soil texture), EC_a, and CI were considerably different in each MLRA and across all fields (table 2). The mean of BD was similar (1.46 Mg m^{-3}) within each MLRA and across all fields. The EC_a levels were higher for fields 1, 2, and 3 (MLRA 113, Central Claypan Areas), as is typical of claypan soils (Sudduth et al., 2003). The EC_a and CI levels were lower for field 4 (MLRA 115B, 22 mS m^{-1}, 1965 kPa) than for MLRA 113 (36 mS m^{-1}, 2430 kPa). The mean TOC was lower (0.86%) for MLRA 115B than for MLRA 113 (1.07%) or

across all fields (1.00%). The mean values of WC and clay content were also lower (25.45% and 31.56%, respectively) for MLRA 115B than for MLRA 113 or averaged across all fields.

Table 2. Means and standard deviations (SD) of field-collected sensor data and laboratory-determined soil properties.

Soil property	Field 1		Field 2		Field 3		Field 4 (MLRA 115B) [a]		MLRA 113		All fields	
	Mean	SD	Mean	SD	Mean	SD	Mean	SD	Mean	SD	Mean	SD
BD (Mg m^{-3})	1.42	0.11	1.48	0.15	1.50	0.12	1.46	0.09	1.46	0.13	1.46	0.12
TOC (%)	1.11	0.54	1.31	0.80	0.90	0.42	0.86	0.54	1.07	0.59	1.00	0.58
WC (%)	29.05	3.41	26.06	4.36	27.65	5.26	25.45	2.76	27.92	4.51	27.04	4.15
Clay (%)	33.21	11.38	35.95	8.43	34.79	11.53	31.56	9.63	34.35	10.96	33.36	10.59
Silt (%)	60.10	11.92	58.29	7.34	58.60	9.90	61.19	11.66	59.17	10.41	59.89	10.92
Sand (%)	6.69	4.40	5.76	2.93	6.62	5.89	7.25	5.43	6.47	4.79	6.75	5.04
CI (kPa)	2292	860	2580	628	2512	425	1956	997	2430	695	2273	846
EC_a (mS m^{-1})	28.18	16.70	48.60	19.44	38.56	15.73	22.38	8.91	36.04	18.66	31.16	17.11
Nobs [b]	24		11		20		30		55		85	

[a] Field 4 was the only one in MLRA 115B; Fields 1, 2, and 3 were in MLRA 113.
[b] Nobs is number of observations.

Soil texture fractions (clay, silt, and sand fractions) for the two MLRAs were generally fine-textured, with low sand content and high silt and clay content (figure 3). An exception was that two points in MLRA 115B had higher sand and clay contents and lower silt.

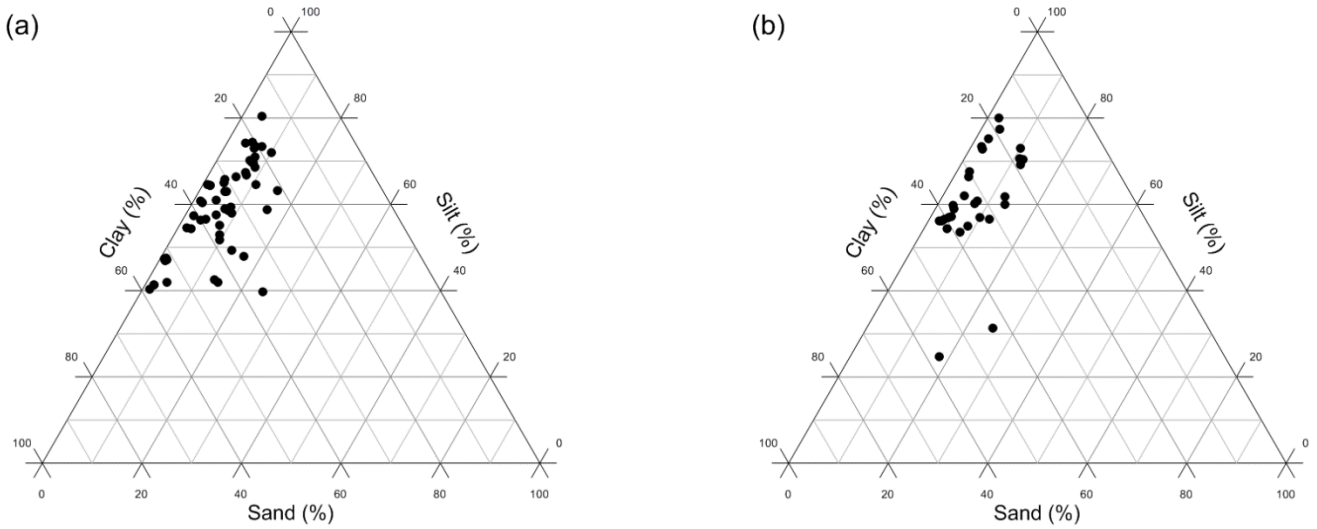

Figure 3. Texture triangles showing clay, silt, and sand content in the soil samples from (a) MLRA 113 and (b) MLRA 115B.

Soil property estimation using PLS analysis of VIS-NIR data

Table 3 shows the cross-validated PLS results for the profile soil analysis at using the full wavelength range (402-2220 nm). In a previous study comparing full and partial wavelength ranges, Cho and Sudduth (2015) determined the full wavelength range of the P4000 provided the best estimation of soil properties. In this study, few soil properties were estimated with good accuracy. In fact, the only entry in that category was silt content in MLRA 115B (RPD = 2.2 and R^2 = 0.81, meeting both the R^2 and RPD criteria. Estimations of BD, WC, and sand fraction were poor (R^2 < 0.50 or RPD < 1.4) for all fields. Estimations of TOC, clay, and silt content met the "fair" RPD and R^2 criteria (R^2: 0.61–0.67;

RPD: 1.58–1.73) for the all-fields dataset. Soil property estimates for MLRA 113 followed trends similar to the all-fields dataset. However, for MLRA 115B, soil texture fraction estimates were more accurate that for the all-fields dataset, with RPD increases ranging from 0.27 to 0.62. These texture fraction estimates for MLRA 115B were near the “good” level defined in previous research.

Table 3. PLS cross-validation statistics for analyses of data from the total soil profile.

Soil property	All fields				MLRA 113				MLRA 115B			
	NPF [a]	R^2_V [b]	RMSEP [c]	RPD	NPF	R^2_V	RMSEP	RPD	NPF	R^2_V	RMSEP	RPD
BD	9	0.32	0.10	1.20	2	0.20	0.11	1.12	1	0.36	0.08	1.22
TOC	5	0.67	0.34	1.73	2	0.64	0.36	1.62	1	0.53	0.38	1.42
WC	8	0.40	3.23	1.29	8	0.34	3.66	1.23	3	0.17	2.46	1.12
Clay	11	0.65	6.36	1.66	10	0.59	7.11	1.54	4	0.76	5.00	1.93
Silt	11	0.61	6.93	1.58	9	0.60	6.70	1.56	8	0.81	5.30	2.20
Sand	7	0.38	4.00	1.26	16	0.48	3.41	1.41	14	0.61	3.37	1.61

[a] NPF is number of PLS factors
[b] R^2_V is R^2 of validation.
[c] Units for RMSEP are given in table 2 for each soil property.

Figure 4 shows scatter plots of reflectance-estimated BD, TOC, WC, and clay content for the all-fields (left), MLRA 113 (center), and MLRA 115B (right) datasets. The best estimates of TOC were for the all-fields dataset (RPD = 1.73) and the best estimates of clay content were in the MLRA 115B dataset (RPD = 1.93). Estimates of BD (RPD = 1.12–1.22) and WC (RPD = 1.12–1.29) were similar within each MLRA and across all fields.

Soil property estimation using PLS with all sensor data

Table 4 shows results of the PLS regression for soil properties (BD, TOC, and WC) from the all-fields, MLRA 113, and MLRA 115B datasets when using different combinations of EC_a, CI and VIS-NIR spectral reflectance as the independent variables. For BD across all fields, the best results were obtained using only VIS-NIR data. In MLRA 113, BD results were improved by adding EC_a to the VIS-NIR data; however, adding CI did not provide additional improvement (table 4). In contrast, the best BD results for MLRA 115B were obtained when using all sensor variables -- VIS-NIR, EC_a, and CI. Estimates of TOC and WC across all fields were better than those for each MLRA regardless of the set of independent variables used. Overall, the best TOC results were obtained with the combination of VIS-NIR and EC_a, while the best WC results were with the combination of VIS-NIR, EC_a, and CI. For most soil properties (BD, TOC, and WC), however, there were generally similar results with reflectance alone and when adding CI or EC_a as independent variables.

Estimates of each soil texture fraction obtained within each MLRA were most accurate when using all sensor variables (table 5). Best results were obtained in MLRA 115B, where estimation of soil texture fractions using all soil sensors reduced RMSEP by approximately 26% for clay, 14% for silt, and 18% for sand content compared to VIS-NIR reflectance alone. The combination of VIS-NIR and CI resulted in largest values of R^2 (0.70) and smallest values of RMSEP (5.92%) for soil clay content across all fields. This combination also provided the best sand content estimates in the all-fields dataset, while the best silt content estimates were obtained with VIS-NIR alone. These texture estimation results were similar to those reported by Wetterlind et al. (2015) who estimated soil texture with errors of approximately 6% for clay and silt, and 10–11% for sand content at the two farms studied. They reported that adding EC_a to VIS-NIR data improved texture estimates, but the level of improvement was small enough that the additional complexity involved with incorporating the additional sensors might not be justified.

Of the sensors on the P4000, VIS-NIR reflectance was the most effective for estimating soil data (BD, TOC, WC, and texture fractions) in this study. This is consistent with Wetterlind et al. (2015), who reported that VIS-NIR was the best individual sensor for soil organic matter and texture variables in their study. Addition of EC_a and CI provided a variable level of improvement ranging from essentially zero up to approximately 26%. This lack of consistency is also consistent with the results of Wetterlind et al. (2015). Additional studies should explore more effective use of the EC_a and CI data, through examination of additional data fusion methodologies, estimation of additional soil properties, and incorporation of data collected over more widely varying soils.

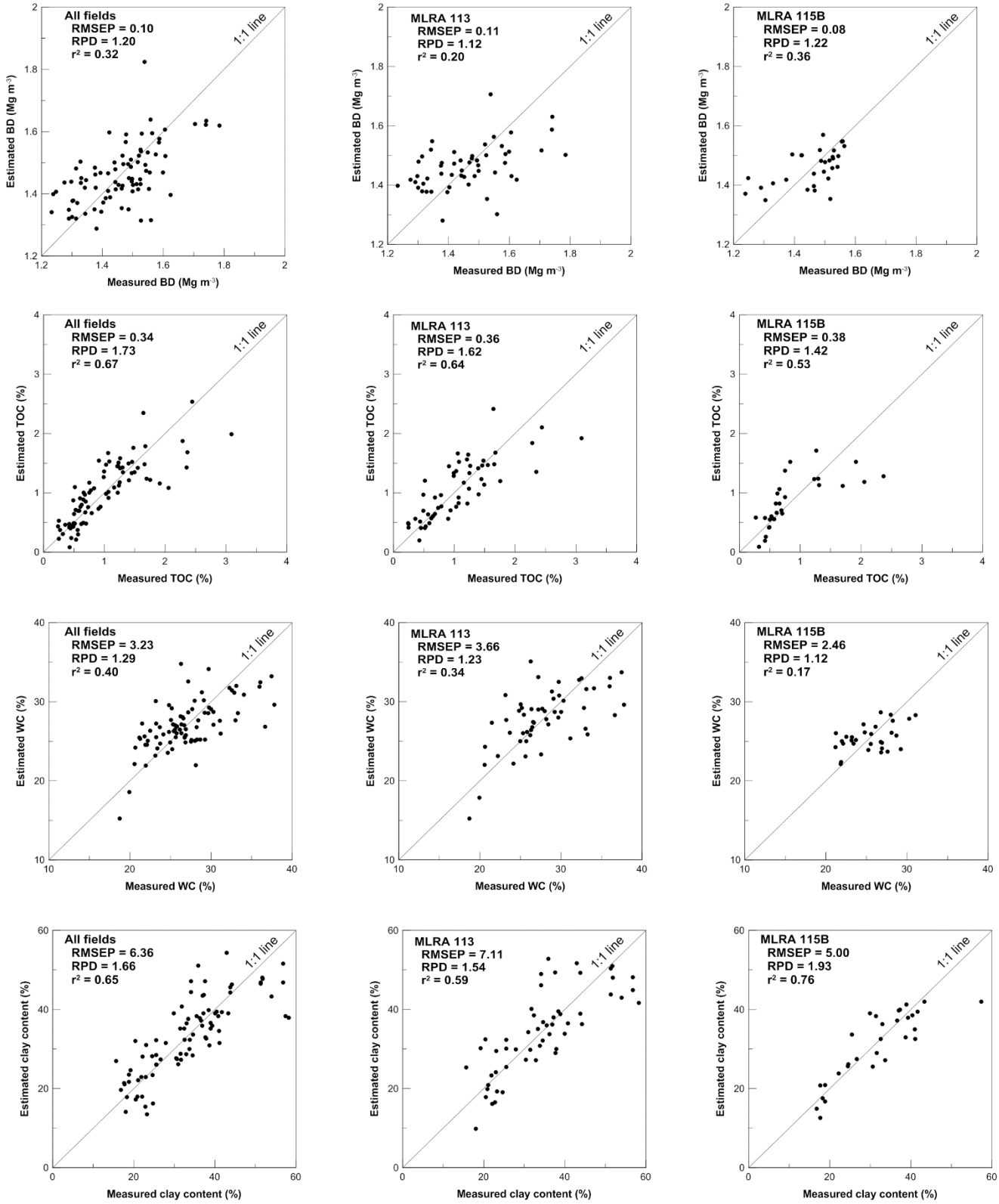

Figure 4. Scatter plots of VIS-NIR PLS-estimated vs. measured values of BD, TOC, WC and clay content for the all-fields (left), MLRA 113 (center), and MLRA 115B (right) datasets.

Table 4. PLS cross-validation statistics for analyses of bulk density (BD), total organic carbon (TOC), and water content (WC) data from all fields, MLRA 113, and MLRA 115B.

Soil property	All fields			MLRA 113			MLRA 115B		
Sensor Variable	R^2_V [a]	RMSEP [b]	RPD	R^2_V	RMSEP	RPD	R^2_V	RMSEP	RPD
BD									
EC_a	0.11	0.11	-	0.21	0.11	-	-	-	-
CI	0.08	0.11	-	0.09	0.12	-	-	-	-
EC_a + CI	0.16	0.11	-	0.28	0.11	-	0.16	0.09	-
VIS-NIR	0.32	0.10	1.20	0.20	0.11	1.12	0.36	0.08	1.22
VIS-NIR + EC_a	0.29	0.10	1.16	0.31	0.11	1.20	0.47	0.07	1.32
VIS-NIR + CI	0.27	0.10	1.16	0.23	0.11	1.14	0.34	0.08	1.21
VIS-NIR + EC_a + CI	0.27	0.10	1.15	0.31	0.11	1.19	0.53	0.07	1.25
TOC									
EC_a	0.19	0.52	-	0.35	0.47	-	0.16	0.49	-
CI	0.12	0.54	-	0.28	0.50	-	-	-	-
EC_a + CI	0.23	0.52		0.39	0.47	-	0.24	0.49	-
VIS-NIR	0.67	0.34	1.73	0.64	0.36	1.62	0.53	0.38	1.42
VIS-NIR + EC_a	0.66	0.34	1.70	0.58	0.39	1.52	0.52	0.39	1.38
VIS-NIR + CI	0.69	0.33	1.78	0.59	0.37	1.58	0.60	0.38	1.42
VIS-NIR + EC_a + CI	0.68	0.33	1.77	0.56	0.38	1.54	0.53	0.40	1.33
WC									
EC_a	- [c]	-	-	-	-	-	-	-	-
CI	-	-	-	-	-	-	-	-	-
EC_a + CI	0.05	4.09	-	-	-	-	-	-	-
VIS-NIR	0.40	3.23	1.29	0.34	3.66	1.23	0.17	2.46	1.12
VIS-NIR + EC_a	0.45	3.06	1.36	0.41	3.50	1.29	0.25	2.60	1.06
VIS-NIR + CI	0.46	3.13	1.33	0.44	3.51	1.29	0.19	2.51	1.10
VIS-NIR + EC_a + CI	0.47	3.04	1.37	0.43	3.53	1.28	-	-	-

[a] R^2_V is R^2 of validation.
[b] Units for RMSEP are given in table 2 for each soil property.
[c] No valid model was possible with this subset of independent variables.

Table 5. PLS cross-validation statistics for analyses of soil texture fractions from all fields, MLRA 113, and MLRA 115B.

Soil texture	All fields			MLRA 113			MLRA 115B		
Sensor Variable	R^2_V [a]	RMSEP [b]	RPD	R^2_V	RMSEP	RPD	R^2_V	RMSEP	RPD
Clay									
EC_a	0.19	9.53	-	0.20	9.82	-	0.10	9.13	-
CI	0.31	8.77	-	0.31	9.08	-	0.32	7.93	-
EC_a + CI	0.39	8.44	-	0.37	8.86	-	0.59	6.52	-
VIS-NIR	0.65	6.36	1.66	0.59	7.11	1.54	0.76	5.00	1.93
VIS-NIR + EC_a	0.63	6.48	1.63	0.58	6.92	1.58	0.73	4.94	1.95
VIS-NIR + CI	0.70	5.92	1.79	0.56	7.29	1.50	0.83	4.01	2.40
VIS-NIR + EC_a + CI	0.66	6.19	1.71	0.64	6.78	1.62	0.85	3.72	2.59
Silt									
EC_a	0.09	10.40	-	0.13	9.70	-	- [c]	-	-
CI	0.14	10.13	-	0.13	9.70	-	0.08	11.19	-
EC_a + CI	0.19	9.96	-	0.20	9.47	-	0.25	10.44	-
VIS-NIR	0.61	6.93	1.58	0.60	6.70	1.56	0.81	5.30	2.20
VIS-NIR + EC_a	0.53	7.56	1.44	0.52	7.40	1.41	0.84	4.92	2.37
VIS-NIR + CI	0.56	7.39	1.48	0.58	6.99	1.49	0.84	4.92	2.37
VIS-NIR + EC_a + CI	0.56	7.41	1.47	0.61	6.67	1.56	0.88	4.57	2.55
Sand									
EC_a	0.01	5.02	-	-	-	-	-	-	-
CI	0.06	4.88	-	0.12	4.49	-	-	-	-
EC_a + CI	0.10	4.84	-	0.17	4.45	-	-	-	-
VIS-NIR	0.38	4.00	1.26	0.48	3.41	1.41	0.61	3.37	1.61
VIS-NIR + EC_a	0.37	4.12	1.22	0.69	2.73	1.76	0.62	3.44	1.58
VIS-NIR + CI	0.39	3.99	1.26	0.54	3.26	1.47	0.72	2.71	2.01
VIS-NIR + EC_a + CI	0.38	4.00	1.26	0.70	2.63	1.82	0.77	2.77	1.96

[a] R^2_V is R^2 of validation.
[b] Units for RMSEP are given in table 2 for each soil property.
[c] No valid model was possible with this subset of independent variables.

Conclusion

Across all four fields in this study, the Veris P4000 VIS-NIR-EC-force probe estimated soil bulk density (BD), total organic carbon (TOC), water content (WC), and soil texture fractions with validation R^2 (and RPD) of 0.32 (1.20) for BD, 0.67 (1.73) for TOC, 0.40 (1.29) for WC, 0.65 (1.66) for clay content, 0.61 (1.58) for silt content, and 0.38 (1.26) for sand content, using VIS-NIR reflectance data alone. Adding EC_a and CI data to spectral reflectance improved WC estimates (R^2 = 0.47, RPD = 1.37). However, there was little to no improvement in estimates of BD, TOC, and texture fractions when adding EC_a and CI data for the all-fields dataset.

For analyses conducted within each MLRA, fusion of data from all three sensors improved some soil texture fraction estimates compared to VIS-NIR data alone. Within MLRA 113, sand content estimates were improved from the poor range (R^2 = 0.48, RPD = 1.41) to the fair range (R^2 = 0.70, RPD = 1.82) by adding CI and EC_a as candidate variables. Within MLRA 115B clay and sand fraction estimates were improved from the fair to the good category. Within MLRA 115B adding CI and EC_a as candidate variables reduced RMSEP by approximatively 26% for clay, 14% for silt, and 18% for sand content compared to VIS-NIR reflectance alone. Additional studies with larger datasets are needed to validate the results from this study and to further investigate calibration improvements possible by fusing multiple sensor datasets.

Acknowledgements and Disclaimer

We thank Tammy Horton, Brent Myers, Kurt Holiman, and Bob Mahurin for assistance with field data collection. We also thank Scott Drummond for assistance with data processing.

Mention of trade names or commercial products in this publication is solely for the purpose of providing specific information and does not imply recommendation or endorsement by the U.S. Department of Agriculture or the University of Missouri.

References

Adamchuk, V. I., Viscarra Rossel, R. A., Sudduth, K. A., & Schulze Lammers, P. (2011). Sensor fusion for precision agriculture. In C. Thomas (Ed.), *Sensor Fusion – Foundation and Applications.* (pp. 27– 40), Rijeka, Croatia: InTech.

ASAE Standards. (2005). S313.3: Soil cone penetrometer. St. Joseph, Mich.: ASAE.

Askari, M. S., Cui, J. F., O'Rourke, S. M., & Holden, N. M. (2015). Evaluation of soil structural quality using VIS–NIR spectra. *Soil and Tillage Research,* 146(A), 108–117.

Barnes, R. J., Dhanoa, M. S., & Lister, S. J. (1989). Standard normal variate transformation and de-trending of near-infrared diffuse reflectance spectra. *Applied Spectroscopy,* 43(5), 772-777.

Chang, C. W., & Laird, D. A. (2002). Near-infrared reflectance spectroscopic analysis of soil C and N. *Soil Science,* 167(2), 110-116.

Chang, C. W., Laird, D. A., Mausbach, M. J., & Hurburgh, C. R. (2001). Near–infrared reflectance spectroscopy-principal components regression analyses of soil properties. *Soil Science Society of America Journal,* 65(2), 480–490.

Cho, Y., Sudduth, K. A., & Chung S. O. (2014). Estimation of soil physical properties from sensor-based soil strength and apparent electrical conductivity. ASABE Paper No. 141914006. St. Joseph, Mich.: ASABE.

Cho, Y., & Sudduth, K. A. (2015). Estimation of soil profile physical and chemical properties using a VIS-NIR-EC-force probe. ASABE Paper No. 152189140. St. Joseph, Mich.: ASABE.

Christy, C., Drummond, P., Kweon, G., Maxton, C., Drelling, K., Jensen, K., & Lund, E. (2011). Multiple sensor system and method for mapping soil in three dimensions. U.S. Patent No. US 20110106451 A1.

Chung, S. O., Sudduth, K. A., Plouffe, C., & Kitchen, N. R. (2008). Soil bin and field tests of an on-the-go soil strength profile sensor. *Transactions of the ASABE,* 51(1), 5-18.

Elbanna, E. B., & Witney, B. D. (1987). Cone penetration resistance equation as a function of the clay ratio, soil moisture content and specific weight. *Journal of Terramechanics,* 24(1), 41–56.

Gee, G. W. & Bauder, J. W. (1986). Particle-size analysis. In A. Klute (Ed.), *Methods of soil analysis. Part 1. Physical and mineralogical methods*. (pp 383–411), Madison, WI: Soil Science Society of America, American Society of Agronomy.

Hodge, A. M., & Sudduth, K. A. (2012). Comparison of Two Spectrometers for Profile Soil Carbon Sensing. ASABE Paper No. 121338240. St. Joseph, Mich.: ASABE.

Koolen, A. J., & Kuipers, H. (1983). *Agricultural Soil Mechanics.* Berlin, Germany: Springer–Verlag.

Kusumo, B. H., Hedley, C. B., Hedley, M. J., Hueni, A., Tuohy, M. P., & Arnold, G. C. (2008). The use of diffuse reflectance spectroscopy for in situ carbon and nitrogen analysis of pastoral soils. *Australian Journal of Soil Research,* 46(7), 623–635.

Kweon, G., Lund, E., Maxton, C., Drummond, P. & Jensen, K. (2008). In situ measurement of soil properties using a probe-based VIS-NIR spectrophotometer. ASABE Paper No. 084399. St. Joseph, Mich.: ASABE.

Lee, K. S., Lee, D. H., Sudduth, K. A., Chung, S. O., Kitchen, N. R., & Drummond, S. T. (2009). Wavelength identification and diffuse reflectance estimation for surface and profile soil properties. *Transactions of the ASABE,* 52(3), 683–695.

Lund, E. D., Christy, C. D., & Drummond, P. E. (1999). Practical applications of soil electrical conductivity mapping in Precision Agriculture. In *Proc. 2nd European Conf. on Precision Agriculture* (pp. 771–779). Sheffield, U.K.: Sheffield Academic Press.

Matney, T., Barrett, L. R., Dawadi, M. B., Maki, D., Maxton, C., Perry, D. S., Roper, D. C., Somers, L., & Whitman, L. G. (2014). In situ shallow subsurface reflectance spectroscopy of archaeological soils and features: a case-study of two Native American settlement sites in Kansas. *Journal of Archaeological Science,* 43,315–324.

McNeill, J. D. (1992). Rapid, accurate mapping of soil salinity by electromagnetic ground conductivity meters. In Topp, G. C., Reynolds, W. D., & Green, R. E. (Eds.), *Advances in measurement of soil physical properties: Bringing theory into practice,* (pp. 209–229), Madison, WI: SSSA.

Morgan, C. L. S., Waiser, T. H., Brown, D. J., & Hallmark. C. T. (2009). Simulated in situ characterization of soil organic and inorganic carbon with visible near-infrared diff use reflectance spectroscopy. *Geoderma,* 151(3–4), 249–256.

Mouazen, A. M., Maleki, M. R., De Baerdemaeker, J., & Ramon, H. (2007). On-line measurement of some selected soil properties using a VIS-NIR sensor. *Soil and Tillage Research,* 93(1), 13–27.

Mulqueen, J., Stafford, J. V. & Tanner, D. W. (1977). Evaluating penetrometers for measuring soil strength. Journal of Terramechanics, 14(3), 137–151.

Myers, D. B., Kitchen, N. R., Sudduth, K. A., Grunwald, S., Miles, R. J., Sadler, E. J., & Udawatta, R. (2010). Combining proximal and penetrating soil electrical conductivity sensors for high resolution digital soil mapping. In Viscarra Rossel, R.A., McBratney, A.B., & Minasny B. (Eds.), *Proximal Soil Sensing,* (pp. 233–243). New York, NY: Springer-Verlag.

Nelson, D. W., & Sommers, L. E. (1996). Total carbon, organic carbon, and organic matter. In Sparks, D. L., Page, A. L., Helmke, P. A., Loeppert, R. H., Soltanpour, P. N., Tabatabai, M. A., Johnston, C. T., & Sumner, M. E. (Eds.), *Methods of Soil Analysis: Part 3, Chemical Methods,* (pp. 961–1010). Madison, WI: SSSA.

Piikki, K., Wetterlind, J., Söderström, M. & Stenberg, B. (2014). Three-dimensional digital soil mapping of agricultural fields by integration of multiple proximal sensor data obtained from different sensing methods. *Precision Agriculture,* 16(1), 29–45.

Rhoades, J. D., Manteghi, N. A., Shrouse, P. J., & Alves, W. J. (1989). Soil electrical conductivity and soil salinity: new formulations and calibrations. *Soil Science Society of America Journal,* 53(2), 433–439.

Saeys, W., Mouazen, A. M. & Ramon, H. (2005). Potential for onsite and online analysis of pig manure using visible and near-infrared reflectance spectroscopy. *Biosystems Engineering,* 91(4), 393–402.

Shepherd, K. D., & Walsh, M. G. (2002). Development of reflectance spectral libraries for characterization of soil properties. *Soil Science Society of America Journal,* 66(3), 988-998.

Sudduth, K. A. & Hummel, J. W. (1993). Soil organic matter, CEC, and moisture sensing with a portable NIR spectrophotometer. *Transactions of the ASAE*, 36(6), 1571–1582.

Sudduth, K. A., Hummel, J. W., & Drummond, S. T. (2004). Comparison of the Veris Profiler 3000 to an ASAE-standard penetrometer. *Applied Engineering in Agriculture,* 20(5), 535–541.

Sudduth, K. A., Kitchen, N. R., Bollero, G. A., Bullock, D. G., & Wiebold, W. J. (2003). Comparison of electromagnetic induction and direct sensing of soil electrical conductivity, *Agronomy Journal,* 95, 472-482.

Sudduth, K. A., Myers, D. B., Kitchen, N. R., & Drummond, S. T. (2013). Modeling soil electrical conductivity–depth relationships with data from proximal and penetrating EC_a sensors. *Geoderma,* 199, 12–21.

The Unscrambler. 2014. Multivariate data analysis simplified. Ver. 10.3: CAMO Technologies Inc. Retrieved from http://www.camo.com/resources/multivariate-types-methods.html. Accessed 12 May 2016.

U.S. Department of Agriculture, 1981. *Land Resource Regions and Major Land Resource Areas of the United States.* USDA-SCS Agricultural Handbook 296. U.S. Government Printing Office, Washington, DC.

Viscarra Rossel, R. A., Walvoort, D. J. J., McBratney, A. B., Janik, L. J. & Skjemstad, J. O. (2006). Visible, near infrared, mid infrared or combined diffuse reflectance spectroscopy for simultaneous assessment of various soil properties. *Geoderma,* 131(1–2), 59–75.

Wetterlind, J., Piikki K., Stenberg B., & Söderström, M. (2015). Exploring the predictability of soil texture and organic matter content with a commercial integrated soil profiling tool. *European Journal Soil Science*, 66(4), 631-638.